The Effect of pH on the Morphology of Electrochemically-grown Polypyrrole Films: An AFM Study

U. Paramo-Garcia[1,2], N. Batina[1], J. G. Ibanez[3,]*

[1] Lab. de Nanotecnología e Ing. Molecular, Área de Electroquímica, Depto. de Química, CBI, Universidad Autónoma Metropolitana-Iztapalapa, Av. San Rafael Atlixco 186, Col. Vicentina, 09340 México D.F. MEXICO
[2] División de Estudios de Posgrado e Investigación, Instituto Tecnológico de Cd. Madero, Juventino Rosas y Jesús Ureta S/N, Col. Los Mangos, 89440 Cd. Madero, Tamps., MEXICO
[3] Centro Mexicano de Química Verde y Microescala. Departamento de Ingeniería y Ciencias Químicas, Universidad Iberoamericana, Prol. Paseo de la Reforma 880, Lomas de Santa Fe, 01219 México, D.F. MEXICO
*E-mail: jorge.ibanez@ibero.mx

Surface changes of electrochemically-grown polypyrrole films on vitreous carbon substrates are analyzed by atomic force microscopy (AFM) as a function of the pH of the source solutions. Thick films are obtained when using H_2SO_4 (i.e., 8.035 µm thick when grown at constant potential, *CP* and 0.157 µm thick when grown by cyclic voltammetry, CV). Such values are estimated from the corresponding areas under the curves either for the *i* vs. *t* (CP) or for the *i* vs. V (CV) plots. PPy films grown at constant potential are thicker than those formed by cyclic voltammetry. In general, film thickness follows essentially the same pattern regardless of the growth technique as a function of pH and of the nature of the anion as follows: SO_4^{2-} (pH = 1) > SO_4^{2-} (pH = 7), Cl^- (pH = 1) > Cl^- (pH = 7). The electrosynthesis potential plays a key role in the final film characteristics, since overoxidation is observed at high applied potentials and promotes considerable stability and conductivity losses.

1. INTRODUCTION

Interest in conducting polymers has grown considerably due to their applications in microelectronic, electrochromic, and biomedical devices, rechargeable batteries, anticorrosion films, chemical and biochemical sensors, protection against electromagnetic radiation, antistatic packaging and the like [1-7]. Modern developments of new custom-designed polymers that partially or completely replace classical materials abound [8-10]. This is especially true in the field of conductive

polymers like polypyrrole, which can be produced electrochemically in the simple way [6,7]. More importantly, electrochemically prepared films can be tailor-made with regards to   thickness, morphology, and conductivity [6,7,11,12]. The overall film properties depend on preparation parameters such as temperature, concentrations, current density, potential, electrode materials, supporting electrolyte, and the nature of anions incorporated into the polymer during the electrosynthesis (dopants) [13-19].

In addition to its traditional uses, polypyrrole has recently emerged as a promising candidate material for various uses in biomedical applications [20-22], especially in neural studies and as scaffold material for nerve regeneration [23,24]. In order to use PPy as biocompatible material one has to be aware that its interactions with live tissue highly depend on polymer surface characteristics such as charge, topography, and roughness, which in turn depend on the synthesis conditions. Some biological functions can be dramatically enhanced by biomaterials with controlled organization at the nanometer scale [25-28].

Taking into consideration such recent interest in using the PPy films for biomedical applications and the fact that the morphology and pH are critical parameters here, in the present work we contribute to the study of the different morphologies of electrochemically-grown films either at constant potential, *CP* or by cyclic voltammetry, *CV* in the presence of various doping ions as a function of the pH of the source solutions (i.e., acidic or neutral values).

2. EXPERIMENTAL PART

A conventional three electrode cell was used for the electrochemical production of PPy films either by *CP* or by *CV*. Vitreous carbon served as the working electrode (WE) (Bioanalytical Systems, MF-2012 minidisk, or The Electrosynthesis, Co., GICR-10 rod, 0.07 cm^2) that was sequentially polished with 0.10 and 0.05 μm alumina, followed by sonication in distilled water for 10-15 min (Branson ultrasound system, 2510R-MT). A Pt wire was used as the auxiliary (counter) electrode. All potentials are referred to an Ag/AgCl$_{(sat)}$ reference electrode (BAS, MF-2052) separated from the medium by a porous Vycor membrane. All the experiments were performed with a BAS potentiostat (Bioanalytical Systems, Model CW50W) at room temperature.

Solutions of H_2SO_4, K_2SO_4, HCl or KCl (J. T. Baker, reagent grade) were used as electrolytes. The pyrrole monomer (Py, Aldrich, 98% reagent grade) was vacuum distilled and stored under a nitrogen atmosphere. All the solutions were prepared with Millipore water (18.2 MΩ at 22.7 ^{o}C) and deareated during 10-15 min with pure nitrogen (Praxair, 99.99%) before performing each experiment.

3. RESULTS AND DISCUSSION

3.1. CP and CV PPy electrosynthesis in acidic or neutral solutions.

Figure 1 shows the cyclic voltammograms corresponding to the formation of PPy films (during 40 polymerization cycles) in the potential range of -0.3 to 0.9 V vs. Ag/AgCl, in SO_4^{2-} or Cl^- media.

Figures 1-a and 1-b show the PPy film growth in H_2SO_4 or K_2SO_4 solutions. The irreversible oxidation of the Py monomer is observed in both cases at potentials between 0.80 and 0.90 V.
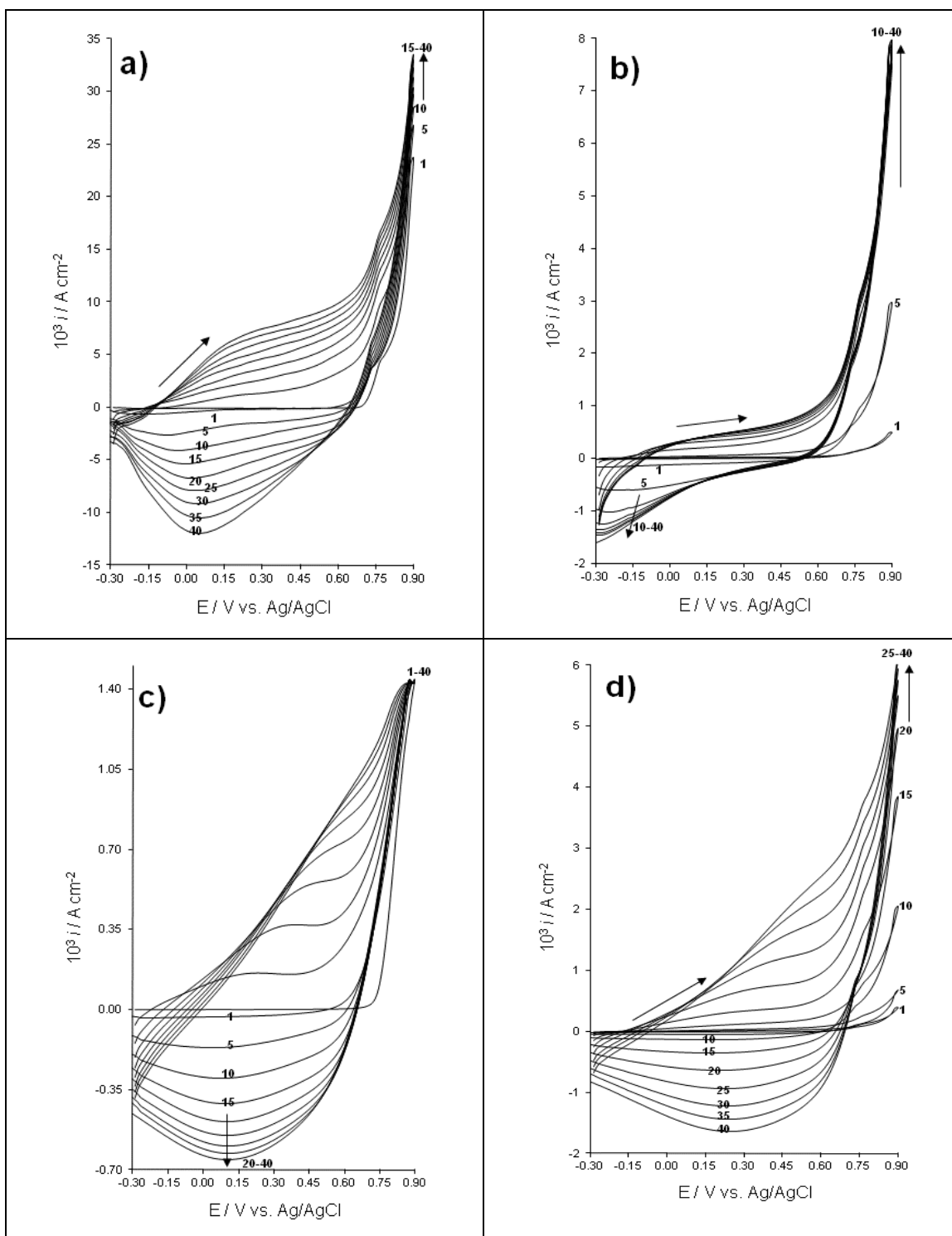

Figure 1. Cyclic voltammetry of the electropolymerization of 0.1 M Py on a vitreous carbon electrode in aqueous medium in the presence of different anions (all at 0.1 M concentration): a) H_2SO_4, b) K_2SO_4, c) HCl, and d) KCl. Each plot comprises 40 cycles between -0.3 and 0.9 V vs. Ag/AgCl at a scan rate = 100 mV/s.

When increasing the number of cycles in Figure 1-a (pH = 1), an irreversible signal appears (-0.15 to 0.450 V) corresponding to the charge-discharge redox process of PPy. On the contrary, at pH = 7 (Figure 1-b) no charge/discharge signal is observed for PPy. This is a clear indication of the poor intrinsic film conductivity. Such observation agrees well with a low degree of anion incorporation into the polymer matrix as observed through its electrochemical behavior [29].

Anodic peaks showing relatively high current densities are observed during PPy film formation in H_2SO_4 and K_2SO_4 (i.e., 33.5 and 7.9 mA cm^{-2}, respectively). Such values are related to the conductivity and amount of polymer deposited on the vitreous carbon substrate, and show that a low solution pH promotes the formation of a thicker film than that formed under neutral conditions.

In HCl (Figure 1-c) and KCl (Figure 1-d) the CV curves show the characteristic signals for PPy electrosynthesis that correspond to the Py monomer oxidation and the polymer charge/discharge irreversible signal described above. In acidic pH (Figure 1-c) the resulting anodic current density is 1.4 mA cm^{-2} whereas that for neutral conditions it is 6.1 mA cm^{-2} (Figure 1-d). Such behavior is contrary to that observed in the SO_4^{2-} system, where at an acidic pH the largest anodic peak is shorter than that at neutral pH. This shows that pH is not the only key factor, but the nature of the dopant ion is important as well.

Figure 2 shows the synthesis of films using a constant potential. The area under each curve is related to the PPy film thickness. When the electrosynthesis potential is increased above 0.80 V (Figure 2-a), the curve shows a current exponential decay which is made more evident at 0.90 V. Such a behavior derives from the well-known PPy film overoxidation.

Figure 2-b shows an exponential decay of the current density at applied potentials greater than 0.85 V. This was not the case when using an acidic pH medium. When comparing Figures 2-a and 2-b at 0.90 V, the area under the curve is evidently greater at the lower pH value. This behavior is similar to that using CV electrosynthesis. In the same manner, overoxidation is facilitated by a greater pH.

Figures 2-c and 2-d show that films formed in HCl and KCl (respectively) are more resistant to overoxidation than those grown in the sulfate electrolytes. This is evident even at 0.95 V for those films grown in HCl. Here, the current response increases with electrolysis time. On the other hand, current stays constant even after 60 s of electrolysis time when using films grown in KCl. This phenomenon has been explained through the formation of hydroxyl and carbonyl groups in the pyrrole ring at high pH values, which decrease the potential required for overoxidation [30,31].

Overoxidation is an irreversible process that involves concomitant structural film changes. This may affect the film´s physical properties like stability and conductivity, and thus preclude their possible use in various applications. Literature estimates indicate that the passage of 1 Coulomb per square centimeter (i.e., 1 C cm^{-2}) is equivalent to a PPy film thickness of 2.5 μm [19,32]. This corresponds to a thickness of 1 μm for the passage of 410 mC cm^{-2} [33] and facilitates the estimation of film thickness. Table 1 shows the thickness of films resulting from the passing of different amounts of charge. The presence of H$^+$ in the electrosynthesis medium favors PPy growth either when using CV or CP. In the same fashion, the amount of charge passed in each case indicates that low pH values favor the formation of more conductive films than those obtained from neutral pH.
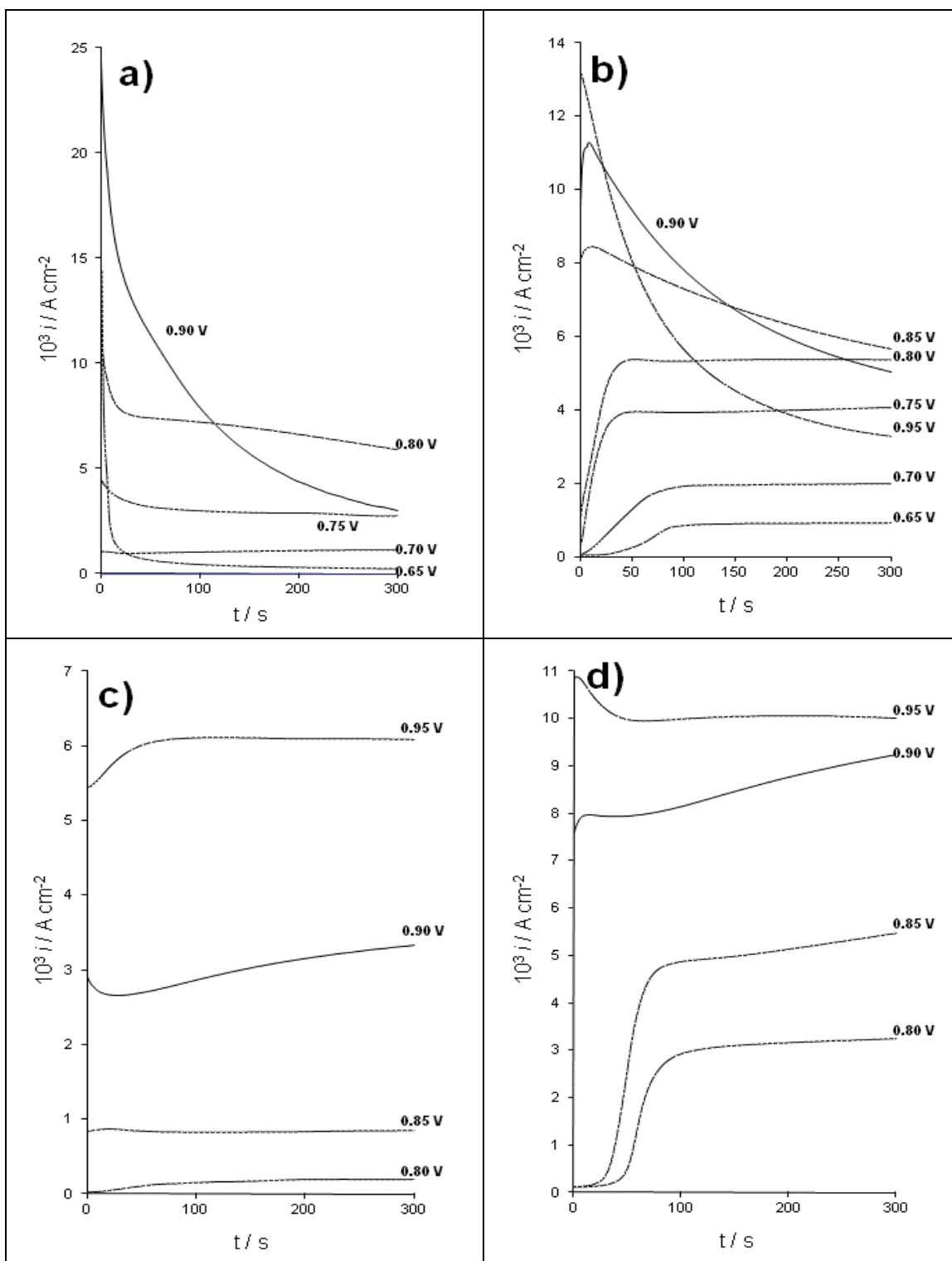
Figure 2. PPy electropolymerization from a 0.1 M Py aqueous solution under constant potential on a vitreous carbon electrode (at pH = 7) in the presence of different anions (all at 0.1 M concentration): a) H_2SO_4, b) K_2SO_4 [29], c) HCl and d) KCl [29]. The current vs. time curves are obtained at 0.9 V vs. Ag/AgCl during 300 s.

These results show that solution pH influences the final thickness of PPy films regardless of the electrochemical technique used. Since PPy films grown at 0.9 V have been used as a reference to study

film morphology by the highly sensitive AFM technique [34], we now proceed to analyze our films using this method.

Table 1. Thickness of PPy films as a function of dopant anion and pH, obtained from PPy film electrosynthesis with different techniques.

Electrolyte	Cyclic voltammetry (-0.3 to + 0.90 V)		Constant potential (0.90 V)			
			t = 20 s		t = 300 s	
	Charge (mC/cm^2)	Thickness (μm)	Charge (mC/cm^2)	Thickness (μm)	Charge (mC/cm^2)	Thickness (μm)
H_2SO_4	62.86	0.157	204.28	0.510	3,214.28	8.035
K_2SO_4	3.77	0.009	123.14	0.307	2,171.43	5.428
HCl	42.85	0.107	118.00	0.295	2,557.14	6.392
KCl	11.20	0.028	60.57	0.151	914.28	2.285

3.2. Atomic Force Microscopy (AFM) study of PPy films grown at constant potential.

In view of the overoxidation effect described earlier, this study was performed by AFM during the initial moments of the electropolymerization process (i.e., 20 s).

Figure 3 shows the top view of a clean vitreous carbon substrate over an area of 2.60 µm x 2.60 µm, using a z-axis interval of 20 nm. The characteristic vitreous carbon morphology of a totally amorphous surface is observed, including rectangular or ellipsoidal nodules or deformations. An analysis of the transversal section in shown in this same figure and yields nodule dimensions (for example, the one in the figure corresponds to a height of 11.931 nm) with areas in the range of 840 to 12,994 nm^2.
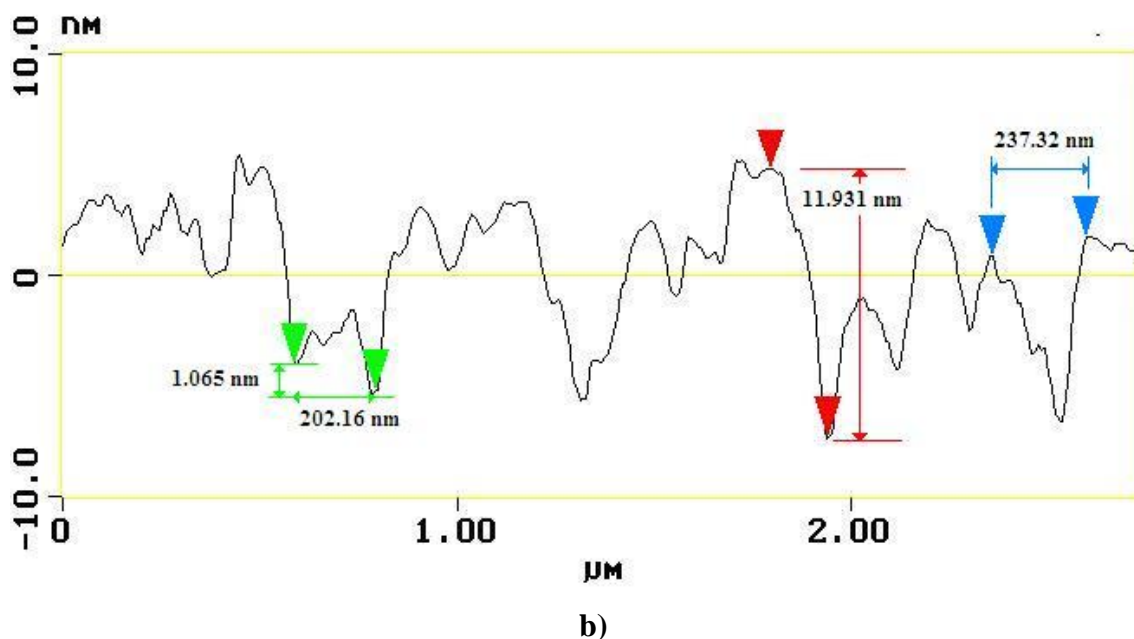

a)

b)
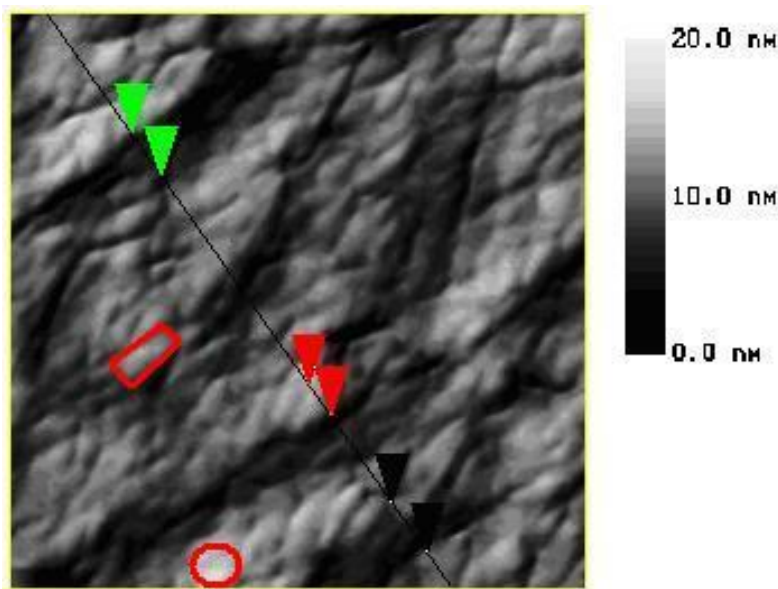
Figure 3. AFM top view (a) and transversal section analysis (b) of a clean vitreous carbon substrate. Area = 2.60 µm x 2.60 µm.

After the clean substrate was characterized, its surface was covered by electropolymerized PPy and the resulting film was observed by AFM (see Figure 4) [16, 17]. Figure 4-a shows the PPy film formed from a H_2SO_4 solution. Large semi elliptical and semi rectangular agglomerations are observed that involve nodular film aggregations resembling the shape of a cauliflower. Their areas are in the range of 39,104 to 506,940 nm^2, and are composed of nodules with areas in the range of 2,463 to 13,273 nm^2.

Figure 4-b shows a PPy film formed from a K_2SO_4 solution. Here, large molecular aggregates with an ill-defined shape are observed. Ellipsoidal forms have an area range of 41,860 to 140,130 nm^2. Outside the aggregates, smaller circular and ellipsoidal nodules range from 11,750 to 25,254 nm^2.

Figure 4-c shows a PPy film formed from an HCl solution. Elliptic and rectangular shapes yield sizes in the range of 5,944 to 136,656 nm^2, although nodules vary widely in size.

Figure 4-d shows a PPy film formed from a KCl solution. Ellipsoidal and rectangular shapes are observed that vary in the range of 5,005 to 134,408 nm^2. The larger irregular mountain-like agglomerates vary widely in size, shape and ordering, and are unevenly dispersed throughout the surface.

Comparison of Figures 4-c and 4-d shows that film morphologies are very similar. However, the film at pH = 1 tends to yield larger particles possibly due to an increase in polymerization rate with $[H^+]$.

A statistical analysis of the PPy surface films permits a quantitative evaluation of their morphologies via determination of their roughness, expressed by the root-mean-square factor, RMS[Rq] [33,35,36]. As a reference, the vitreous carbon substrate yields a [RMS]Rq = 3.62 nm. Figure 5 shows that the roughness values increase with film thickness.
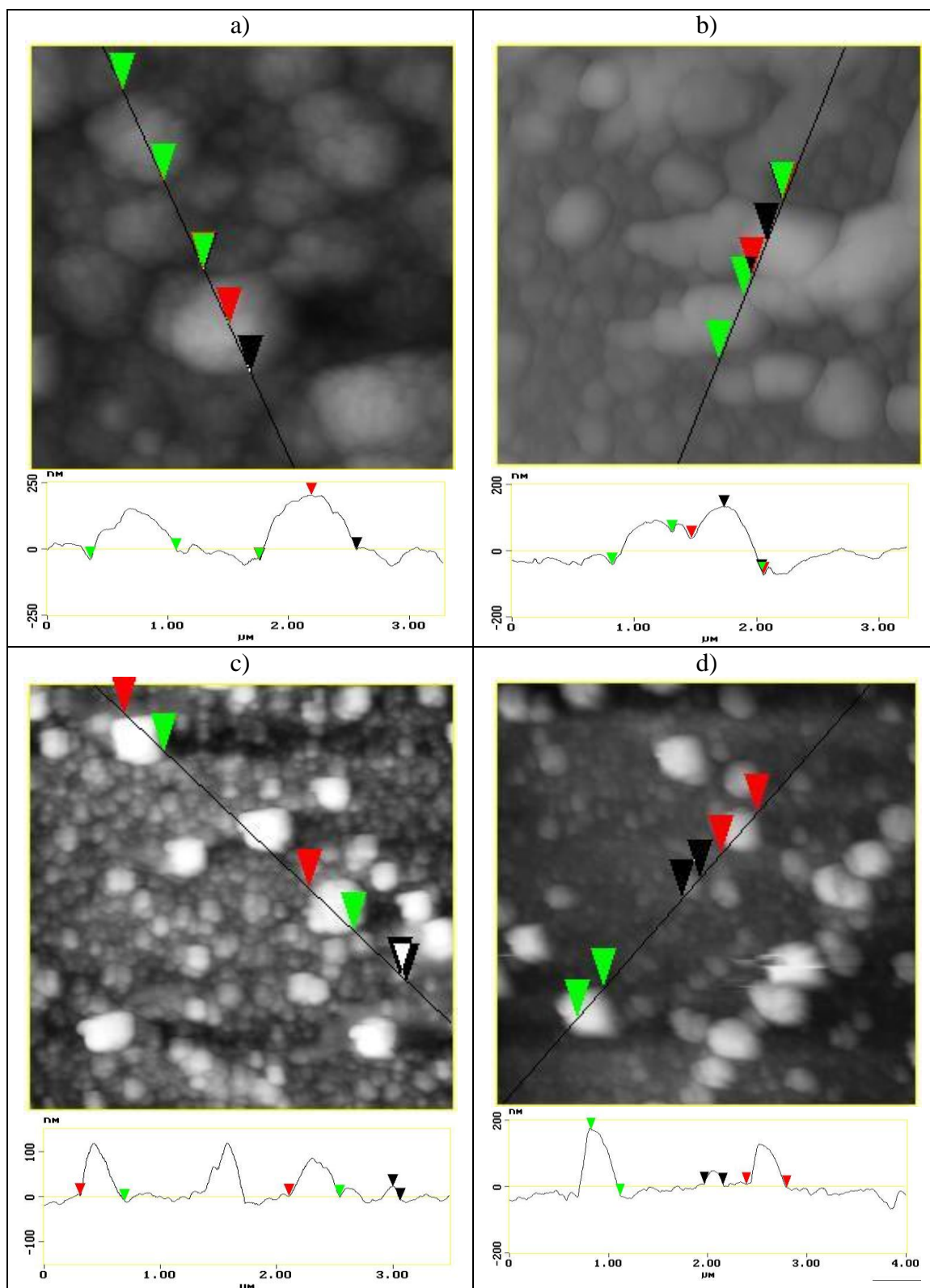
Figure 4. AFM images of PPy films synthesized at a constant potential of 0.90 V vs. Ag/AgCl (during 20 s), in different 0.1 M electrolytes: a) H_2SO_4, b) K_2SO_4, c) HCl, and d) KCl.
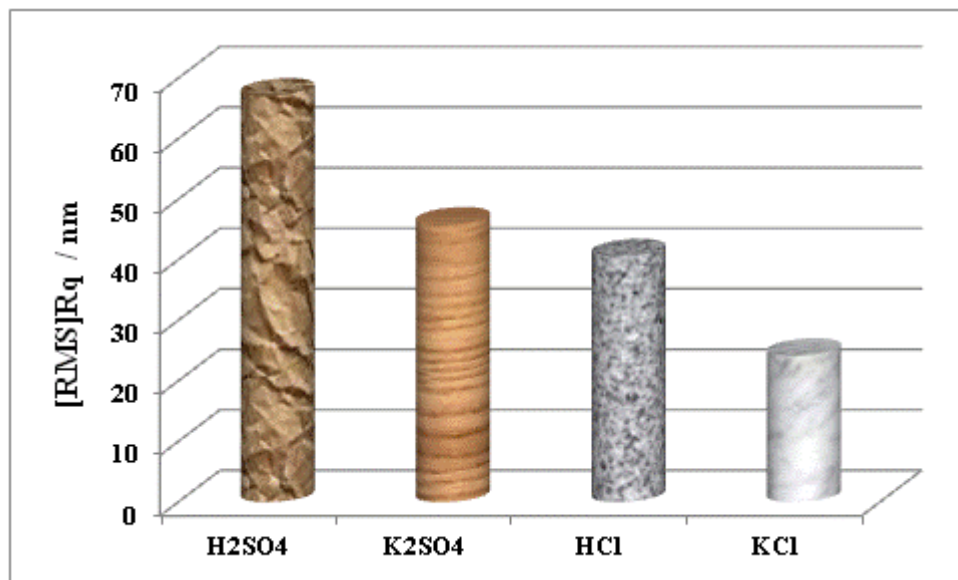
Figure 5. Roughness of PPy films as a function of the nature of the dopant.

4. CONCLUSIONS

PPy films grown at constant potential are thicker than those formed by cyclic voltammetry. Nonetheless, film thickness follows essentially the same pattern regardless of the growth technique as a function of pH and of the nature of the anion as follows: SO_4^{2-} (pH = 1) > SO_4^{2-} (pH = 7), Cl^- (pH = 1) > Cl^- (pH = 7).

Application of high potentials yields overoxidized PPy films. This is evidenced by an exponential current decay for the films grown at constant potential. Higher pH values displace the potential required for overoxidation to more cathodic values. It is clearly shown that in order to produce fine and stable PPy films one should first determine the range of the electrosynthesis potentials in every electrolyte and for each solution pH.

Atomic Force Microscopy (AFM) shows that the topography of the films is affected by the type of ion dopant used during electrosynthesis on a vitreous carbon electrode. The quantitative analysis of the surface roughness of PPy films is of paramount importance when comparing the different surface morphologies. In terms of using PPy films for biomedical applications, key surface roughness and topographic characteristics can now be tailored as they vary with pH and electrodeposition conditions.

References

1.   K. Aydemir, S. Tarkuc, A. Durmus, G. Gunbas and L. Toppare, *Polymer,* 49 (2008) 2029.

2. B. Grgur, M. Gvozdenović, J. Stevanović, B. Jugović and V. Marinović, *Electrochim. Acta,* 53 (2008) 4627.
3. K. Nakahara, J. Iriyama, S. Iwasa, M. Suguro, M. Satoh and E. Cairns, *J. Power Sources,* 165 (2007) 870.
4. S. Carquigny, O. Segut, B. Lakard, F. Lallemand and P. Fievet, *Synth. Met.,* 158 (2008) 453.
5. S. Radhakrishnan and S. Paul, *Sens. Actuators B,* 125 (2007) 60.
6. T. Vernitskaya and O. Efimov, *Russ. Chem. Rev.,* 66 (1997) 443.
7. J. Heinze, B. Frontana-Uribe and S. Ludwigs, *Chem. Rev.,* 110 (2010) 4724.
8. K. Schoch and H. Saunders, *IEEE Spectrum,* 29-6 (1992) 52.
9. G. Fredrickson, *Nature Mat.,* 7 (2008) 261.
10. T. Greef and E. Meijer, *Nature,* 453 (2008) 171.
11. Z. Qi and P. Pickup, *Chem. Mater.,* 9 (1997) 2934.
12. L. Curtin, G. Komplin and W. Pietro, *J. Phys. Chem.,* 92 (1988) 12.
13. T. Raudsepp, M. Marandi, T. Tamm, V. Sammelselg and J. Tam, *Electrochim. Acta*, 53 (2008) 3828.
14. C. Weidlich, K. M. Mangold and K. Juttner, *Electrochim. Acta*, 50 (2005) 1547.
15. J. Wang, Y. Xu, X. Chen, X. Du and X. Li, *Acta Phys-Chim. Sin.,* 23 (2007) 299.
16. S. H. Song, D. S. Han, H. J. Lee, H. S. Cho, S. M. Chang, J. M. Kim and H. Muramatsu, *Synth. Met.*, 117 (2001) 137.
17. A. Hallik, A. Alumaa, H. Kurig, A. Jänes, E. Lust and J. Tamm, *Synth. Met.,* 157 (2007) 1085.
18. R. Bull, R. Fan and A. Bard, *J. Electrochem. Soc.,* 129 (1982) 1009.
19. Z. Qi, N. Rees and P. Pickup, *Chem. Mat*er., 8 (1996) 701.
20. A. Malinauskas, *Polymer* 42 (2001) 3957.
21. A. N. Zelikin, D. Lynn, J. Farhadi, I. Martin, and R. Langer, *Angew. Chem.*, 41 (2002) 141.
22. A. N. Zelikin, V. Shastri, D. Lynn, J. Farhadi, I. Martin and R. Langer, *Mater. Res. Soc. Symp. Proc.*, Boston, MA, 2002.
23. C. E. Schmidt, V. R. Shastri, J. P. Vacanti, R. Langer, *Proc. Nat. Acad. Sci. USA*, 94 (1997), 8948.
24. P. M. George, A. W. Lykman, D. A. La Van, A. Hedge, Y. Lenug, R. Avasare, C. Testa, P. M. Alexander, R. Langer and M. Sur, *Biomater.*, 26 (2005) 3511.
25. A. D. Bendrea, L. Ciang and I. Ciang, *J. Biomater. App.*, 26 (2011) 3.
26. L. Qu, G. Shi, F. Chen and J. Zhang, *Macromolec.*, 36 (2003) 1063.
27. X. Zhang, J. Zhang, W. Song and Z. Liu, *J. Phys. Chem. B.*, 110 (2006) 1158.
28. V. Lundin, A. Heraland, M. Berggren, E. W. H Jager and A. I. Teixeira, *Plos One*, 6 (2011) 1.
29. U. Paramo-Garcia, J. G. Ibanez and N. Batina. *Int. J. Electrochem. Sci.,* 6 (2011) 5172.
30. Y. Li and R. Qian, *Electrochim. Acta*, 45 (2000) 1727.
31. J. Mostany and B. Scharifker, *Electrochim. Acta*, 42 (1997) 291.
32. Y. Wang and K. Rajeshwar, *J. Electroanal. Chem.*, 425 (1997) 183.
33. B. Negler, N. Laxmeshwar and K. Santhanam, *Ind. J. Chem.*, 33A (1994) 547.
34. J. G. Ibanez, A. Alatorre-Ordaz, S. Gutierrez-Granados and N. Batina, *Polym. Degrad. Stabil.,* 93 (2008) 827.
35. E. Chainet and M. Billon, *Synth. Met.,* 99 (1999) 21.
36. A. Kaynak, *Mat. Res. Bull.,* 32 (1997) 271.